

## Research Article

# Selective Electrochemical Determination of Etoposide Using a Molecularly Imprinted Overoxidized Polypyrrole Coated Glassy Carbon Electrode

Hajer Hrichi <sup>1,2</sup>, Lotfi Monser <sup>2</sup>, and Nafaâ Adhoum<sup>2,3</sup>

<sup>1</sup>Chemistry Department, College of Science, Jouf University, P.O. Box: 2014, Sakaka, Saudi Arabia

<sup>2</sup>National Institute of Applied Sciences and Technology, Carthage University, Centre Urbain Nord, B.P. N° 676, 1080 Tunis Cedex, Tunisia

<sup>3</sup>Preparatory School for Engineering Studies, Kairouan University, Tunisia

Correspondence should be addressed to Hajer Hrichi; hahrichi@ju.edu.sa

Received 2 November 2018; Accepted 18 December 2018; Published 2 January 2019

Academic Editor: Shengshui Hu

Copyright © 2019 Hajer Hrichi et al. This is an open access article distributed under the Creative Commons Attribution License, which permits unrestricted use, distribution, and reproduction in any medium, provided the original work is properly cited.

A simple and efficient new electrochemical sensor based on molecularly imprinted polymer has been developed for selective detection of an anticancer agent Etoposide (ETP). The sensor was prepared by electropolymerization via cyclic voltammetry (CV) of pyrrole onto a glassy carbon electrode (GCE) in the presence of ETP molecules. The extraction of ETP molecules embedded in the polymeric matrix was carried out by overoxidation in sodium hydroxide medium using CV. Various important parameters affecting the performance of the imprinted film (MIP) coated sensor were studied and optimized using differential pulse voltammetry (DPV). Under optimal conditions, the sensor response exhibited a linear dependence on ETP concentration ( $R^2 = 0.999$ ) over the range  $5.0 \times 10^{-7}$  M –  $1.0 \times 10^{-5}$  M with a LOD ( $3\sigma/m$ ) of  $2.8 \times 10^{-9}$  M. The precision (% RSD,  $n=6$ ) of the proposed sensor for intra- and interdays was found to be 0.84 and 2.46%, respectively. The selectivity of MIP/GCE sensor toward ETP was investigated in the presence of different interfering molecules including excipients and ETP metabolites. The developed sensor showed great recognition ability toward ETP and was successfully applied for its determination in injectable dosage forms and biological human fluids.

## 1. Introduction

Etoposide (ETP) (4-demethylepipodophyllotoxin ethylidene- b-D-glucoside) is a potent clinical anticancer agent [1]. It is one of the most widely used cytotoxic drugs and has strong antitumour activity against small-cell lung cancer, leukemia, testicular cancer, lymphomas, and a variety of childhood malignancies [2–6]. Both intravenous and oral dosage forms of ETP are used and often given in combination with other antineoplastic drugs of different mode of action like cisplatin [7, 8]. Experimental studies indicated that oral administration of ETP results in variable absorption that averages about 50%. Furthermore, after intravenous injection, an average peak plasma concentration of  $30.0 \mu\text{g mL}^{-1}$  was reported. Besides, it was demonstrated that ETP is about 94% bound to plasma and approximately 40% of an

administered dose is excreted intact in urine [9]. Thus, it is of particular significance to develop sensitive and selective analytical method to monitor the amount of ETP in quality control and biological fluids due to its importance in cancer therapy. Literature research indicated various studies describing several analytical methods for the determination of ETP in many matrices including injectable dosage forms, biological fluids, and cancer cells. These methods are almost based on high-performance liquid chromatography [10–19], spectrofluorimetry [20], and micellar electrokinetic chromatography [21]. However, these methods are time-consuming, demand expensive instrumentation, need complicated sample preparation including extraction and preconcentration, and require an extensive use of organic solvents. Modern electrochemical techniques, in contrast, stand as promising alternatives to classical approaches due to their moderate

operational cost, simplicity, and good miniaturization potential enabling rapid and sensitive drug detection. Since ETP is an electroactive compound, electrochemical methods are one of the most favorable techniques for its determination. As mentioned in the literature surveys, some electrochemical sensors have been employed to determine ETP using different working electrodes such as carbon paste electrode [22], multiwalled carbon nanotube-modified glassy carbon electrode [23], carbon paste electrode based on sepiolite clay [24], glassy carbon electrode modified with oxidized multiwalled carbon nanotubes (oMWCNTs) [25], and glassy carbon electrode modified with carbon quantum dots (CQDs) [26]. Molecular recognition or artificial receptors with molecularly imprinted polymers (MIP) have been a significant tool for the development of electrochemical sensors. These materials have specific advantages in terms of specific recognition ability, low cost of preparation, high stability, high surface-to-volume ratio, and excellent selectivity [27, 28]. Employing MIPs in drug analysis has been extensively investigated for a couple of decades now, as they can be applied to extract only the template molecule. Selectivity and sensitivity could be also remarkably enhanced using electrochemical techniques as detection methods for MIPs based sensors [29]. It was demonstrated that MIP films synthesized *via* electropolymerization have various interesting advantages with respect to adherence to a transducer of any shape and size as well as simplicity and speed of preparation. Likewise, the electropolymerization facilitates easy control of the film thickness and morphology under several deposition conditions [30]. In this study, an electrochemical ETP sensor based on molecularly imprinted overoxidized polypyrrole film deposited on glassy carbon electrode was developed and evaluated. The analytical performances of the modified sensor were studied using differential pulse voltammetry. The proposed sensor has been successfully applied to the analysis of ETP in injectable dosage forms and human biological fluids. To the best of our knowledge, the proposed method is the first application of MIP modified electrochemical sensor for ETP determination.

## 2. Experimental

**2.1. Chemicals.** Unless otherwise stated, all chemicals employed in this work were in guaranteed reagent grade and used without further purification. Etoposide powder, benzyl alcohol, citric acid, polysorbate 80, and macrogol 300 were kindly supplied by the National Laboratory of Drugs Control (Tunisia). Pyrrole (98%),  $\text{NaClO}_4$  ( $\geq 98\%$ ), boric acid ( $\geq 99.5\%$ ), and acetic acid ( $>99\%$ ) were obtained from Sigma-Aldrich (Steinheim, Germany). Sodium hydroxide (99%) and methanol (99.8%) were purchased from Prolabo (France). Britton-Robinson buffer (BRB) solution (0.05 M), used as supporting electrolyte, was prepared by dissolving appropriate amounts of acetic, o-phosphoric, and boric acids in double distilled water. A brand of ETP injection (Etoposide Mylan®) was provided by the National Laboratory of Drugs Control (Tunisia). Stock standard solutions of Etoposide ( $1.0 \times 10^{-3}$  M) were prepared in methanol and stored in the

freezer at  $-18^\circ\text{C}$ . Standard solutions were prepared by diluting the stock solution with BRB solution (0.05 M) and adjusted to the required pH with 0.2 M sodium hydroxide solution. Working standards of ETP were freshly prepared just before assay, by adding appropriate amounts of stock solution directly to the voltammetric cell.

**2.2. Apparatus.** Cyclic voltammetry (CV) and differential pulse voltammetry (DPV) measurements were performed with a VoltaLab 80 potentiostat (Model PGZ 402) and data acquisitions were accomplished using Voltmaster 4 software. The electrochemical measurements were carried out in a classical three-electrode system. A glassy carbon electrode (GCE) was used as a working electrode ( $A = 0.196 \text{ cm}^2$ ), a saturated calomel electrode (SCE) as reference electrode, and a platinum wire as an auxiliary electrode. The surface of GCE was polished using alumina ( $0.05 \mu\text{m}$ ), sonicated successively in acetonitrile-water (1:1, V/V), and then dried at room temperature before its use. The pH measurements of all sample solutions were realized with a Mettler-Toledo 340 pH-meter with an accuracy of 0.01 pH unit and were calibrated with standard buffers at room temperature. Attenuated total reflectance Fourier transform infrared (ATR-FTIR) spectra were recorded on a (PerkinElmer, Model 2000) spectrometer to characterize the imprinted film. The AFM tapping mode images were recorded using an atomic force microscope (model: XE-70, from Park Systems, Korea).

**2.3. Preparation of MIP and NIP Modified Electrodes.** The MIP film was obtained by electropolymerization of pyrrole on the surface of the GCE using cyclic voltammetry (CV) in the potential range between -0.6 and 1.0 V (versus SCE) during four cycles at a scan rate of  $100 \text{ mVs}^{-1}$ . The polymerization mixture includes 0.1 M  $\text{NaClO}_4$ ,  $3.0 \times 10^{-4}$  M ETP, and 0.1 M pyrrole. After electropolymerization, the working electrode was rinsed with double distilled water and the embedded ETP molecules were extracted from the conducting polymer matrix by the overoxidation operation. The GCE was immersed in a 0.1 M sodium hydroxide solution and the overoxidation was carried out using CV in the potential range of 0.8 to 1.2 V for 40 cycles at a scan rate of  $50 \text{ mVs}^{-1}$  until all ETP molecules were stripped from the imprinted polypyrrole matrix. A nonimprinted electrode (NIP) was prepared as above, but without adding ETP to the polymerization mixture in order to check the reliability of the measurements.

**2.4. Analysis of ETP in Injectable Solution and Human Biological Fluids.** Adequate amount of Etoposide Mylan® injectable solution, claimed to contain 20.00 mg ETP per 5.0 mL, was transferred to a 100 mL volumetric flask and dissolved in methanol. Then, the mixture was sonicated for 5 min in an ultrasonic bath. An aliquot of this solution was transferred into a 10.0 mL voltammetric cell, diluted to the volume with 0.05 M BRB of pH 4.0 to get final concentration of ETP within the working range. The content of the injectable solution was quantified using the standard addition method.

Serum and plasma samples, obtained from drug-free human blood, were kindly supplied from the Hospital of the

Internal Security Forces of La Marsa (Tunisia) and stored frozen until assay. The samples were then thawed gently at room temperature and vortexed to ensure homogeneity. An aliquot volume of each biological fluid was spiked with ETP to achieve a required concentration and then treated with 1.0 mL methanol to precipitate plasma proteins effectively. Then, the mixture was centrifuged for 15 min at 5000 rpm and the supernatant was filtered through a 0.45 mm filter (Millipore, Germany) in order to remove the protein bound fraction of the drug. Subsequently, appropriate volumes of the supernatant were transferred into the voltammetric flask and diluted to an appropriate concentration by the addition of an adequate amount of the supporting electrolyte of pH 4.0. The suitability of the developed sensor for analysis of ETP in human urine was also investigated. For this purpose, samples of human urine were collected from a healthy volunteer immediately before the experiments and were centrifuged for 10 min at 4000 rpm. The supernatant was filtered using a 0.45  $\mu\text{m}$  (Millipore, Germany) filter and an aliquot volume of human urine (1.0 mL) was suitably fortified with ETP standard solution to achieve an appropriate concentration. An adequate volume of the fortified supernatant was added to the voltammetric flask and was diluted to 10 mL with the supporting electrolyte. Measurements were carried out by DPV using standard addition method in order to reduce the matrix effect. The selectivity of MIP film against ETP was investigated by testing the DPV response of the modified GCE in the presence of increasing amounts of four interferents: benzyl alcohol, citric acid, polysorbate 80, and macrogol 300. Besides, the selectivity of the MIP sensor was carried out in biological fluids in the presence of two metabolites. ETP quinone and ETP catechol were synthesized according to the procedures described by the patent of Nemeč [31] and the method of Relling [32], respectively.

**2.5. Electroanalytical Measurements.** Current measurements of MIP/GCE sensor were performed using differential pulse voltammetry (DPV) in 0.05 M BRB solution. The voltammograms were recorded in a potential range between 0.00 and 1 V (versus SCE). DPV experiments were performed using the following instrumental parameters: step potential 8 mV, modulation amplitude 50 mV, and scan rate 15  $\text{mVs}^{-1}$ . In a typical run, the modified electrochemical sensors were immersed in a voltammetric cell containing 10 mL of the supporting electrolyte solution. After measurement of the blank solution, an appropriate volume of standard stock solution of ETP was added and after a stirring period of 5 min, differential pulse voltammograms were recorded to investigate the sensing performance. The calibration curve was obtained by spiking the supporting electrolyte with known quantities of ETP standard stock solution and plotting the current intensities against the corresponding ETP concentration. All measurements were made at ambient temperature ( $20 \pm 5^\circ\text{C}$ ).

### 3. Results and Discussion

**3.1. Preparation of Molecularly Imprinted Films.** The electropolymerization of monomer occurred at the surface of

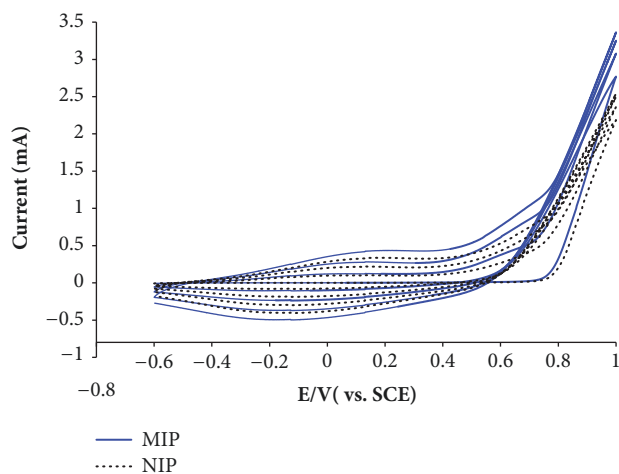


FIGURE 1: Cyclic voltammograms recorded during the formation of the imprinted and nonimprinted polypyrrole films at glassy carbon electrode. Experimental conditions: [pyrrole] = 0.1 M; [ETP] =  $3.0 \times 10^{-4}$  M;  $[\text{NaClO}_4]$  = 0.1 M; number of cyclic scans = 4; scan rate =  $100 \text{ mVs}^{-1}$ .

a GCE immersed in an aqueous solution containing 0.1 M pyrrole, 0.1 M of  $\text{NaClO}_4$ , and  $3.0 \times 10^{-4}$  M of ETP. Cyclic voltammograms were recorded during the electropolymerization process using a potential cycling between -0.6 and 1 V (versus SCE). By increasing the number of cycles, the current intensity increased progressively ensuring that conducting MIP and NIP films are formed and coated onto the GCEs surfaces progressively (Figure 1).

A broad peak observed at about 40 mV for both MIP and NIP modified electrodes was attributed to polypyrrole oxidation. Although the voltammograms corresponding to MIP and NIP formation look similar in shape, an anodic peak corresponding to the oxidation of ETP and appearing at about 0.6 V was exclusively recorded with MIP film. Moreover, the obvious increase of anodic and cathodic current intensities of MIP film in comparison with NIP film reveals the difference of MIP and NIP growth. This behavior was obviously ascribed to the presence of ETP molecules and provided supporting indication on its effective embodiment into the polymer matrix. In this study, electrochemical elution approach was chosen using CV to extract ETP molecules from the polypyrrole matrix and create complementary imprinted sites for the subsequent rebinding. The overoxidation of polypyrrole was regarded as a promising alternative approach that replaces the conventional extraction attempts used while preparing the MIPs [33]. During overoxidation, polypyrrole loses its electroactivity due to the ejection of the dopant (dedoping), and oxygen-containing groups such as carbonyl and carboxyl are introduced to the pyrrole unit [34]. The presence of dense carbonyl groups on the backbone of overoxidized polypyrrole film can afford a selective interface for binding interactions between the polymer and the immobilized template molecule [35]. In addition, it was pointed out that overoxidation has two effects on MIP selectivity: (1) it can eliminate the template molecule to form the complementary cavity, and (2) it can enhance the polymer texture to make the cavity more stable

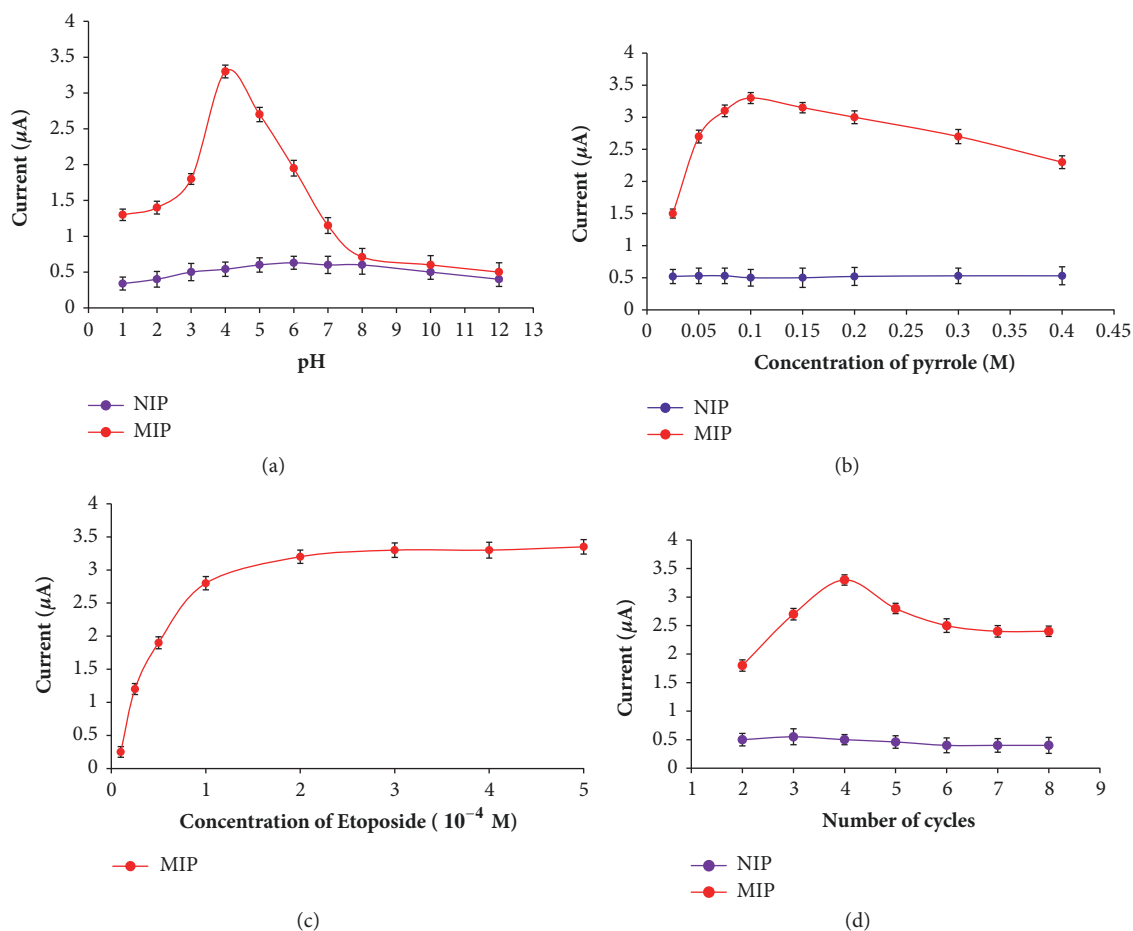


FIGURE 2: (a) The effect of pH of Britton-Robinson buffer solution; (b) pyrrole concentration; (c) ETP concentration; and (d) the number of cycles on MIP and NIP GCE sensitivity. The electroanalytical signal was measured through DPV response to  $5.0 \times 10^{-6}$  M ETP in BRB solution (pH 4.0). Error bars represent the standard deviation of three independent measurements.

[36]. As can be seen in Figure S.1.A (Supplementary Material), successive scan cycles performed during the overoxidation process displayed a decreasing current. This behavior was ascribed to the decrease in conductivity of the polypyrrole film as a result of the electrochemically irreversible overoxidation process [37]. NIP films were also overoxidized under the same conditions as MIP films. The effect of the number of cycles applied during the overoxidation process on the evolution of released ETP molecules was investigated by DPV on an uncovered GCE. The recorded DPV profile (Figure S.1.B, Supplementary Material) exhibited a rapid release of ETP during the first 20 cycles, which then slowed down to reach a plateau from the 40<sup>th</sup> cycle. This result suggests a controlled and complete release of ETP molecules from the polymer matrix during the overoxidation operation. In addition, it was found that the application of 40 cycles during the overoxidation leads to a total stripping of the amount of ETP molecules ( $3.0 \times 10^{-4}$  M) initially introduced in the prepolymerization mixture. Consequently, the extraction cycles were optimal at 40 cycles for complete extraction of ETP from the polypyrrole matrix.

**3.2. Optimization of Operational Parameters.** The main operational parameters including the pH during the DPV analysis, the incubation time, the monomer, template and supporting electrolyte concentrations, and the number of cycles are significant factors affecting the recognition ability of the MIP sensor [38, 39]. In this study, the investigation and optimization of these parameters were realized by a univariate method consisting in comparing MIP and NIP DPV responses.

**3.2.1. Influence of pH.** In order to achieve the highest sensitivity of the MIP/GCE sensor, it is important to discuss the influence of pH of the Britton-Robinson buffer solution on the electrochemical response of ETP. The responses of MIP and NIP modified electrodes were evaluated in BRB solutions containing  $5.0 \times 10^{-6}$  M of ETP while the pH was varied between 2.0 and 12.0. As illustrated in Figure 2(a), differential pulse voltammetric response of ETP increases in the pH range of 1.0–4.0 and then decreases. Such trend can be attributed to the weakness of electrochemical oxidation of ETP at pH > 4.0 [22], inducing a poor interaction between the neutral form of ETP and the overoxidized polypyrrole.

Nevertheless, at a higher pH values ( $>9.0$ ), no differences between the analytical responses of MIP and NIP modified GCEs were observed. This behavior can be ascribed to the weak interaction between the phenolate form of ETP ( $pK_a = 9.8$ ) [40] and the overoxidized polypyrrole film. Consequently, the Britton-Robinson buffer solution of pH 4.0 was chosen as the background electrolyte in this study.

**3.2.2. Influence of Concentrations of Pyrrole Monomer and Supporting Electrolyte in the Prepolymerization Mixture.** To investigate the influence of pyrrole concentration on the response of the modified sensor, several MIP/NIP modified GCEs were prepared by varying pyrrole concentration in the polymerization mixture between 0.025 and 0.4 M. All the rest of operational parameters were kept constant. The analytical performance of each prepared electrode was evaluated by recording its DPV response in the presence of  $5.0 \times 10^{-6}$  M of ETP. Figure 2(b) depicts a net difference between DPV responses of MIP and NIP modified GCE in sensing ETP, confirming the success of the imprinting process. The responses of the MIP/GCE increased significantly, reached maximum with the concentration of 0.1 M, and then decreased with further increasing the concentration of pyrrole. This behavior can be explained by the formation of thicker MIP films, which impede the accessibility of target molecules to the binding sites, reducing the sensitivity of the sensor. As a result, the concentration of pyrrole of 0.1 M was chosen as the optimum for the electropolymerization to obtain the highest sensitivity for the determination of ETP. The concentration of the supporting electrolyte  $\text{NaClO}_4$  is another important parameter that further influences the analytical performance of the modified MIP/GCE sensor. The effect of the concentration of  $\text{NaClO}_4$  on the MIP sensing was investigated over the range from 0.02 M to 0.60 M. The best results were obtained using 0.10 M of  $\text{NaClO}_4$ ; additional increase in the concentration did not intensify the analytical response.

**3.2.3. Influence of the Concentration of Template and the Incubation Time.** The concentration of ETP in the polymerization mixture is another main factor that was studied in our investigation. For this aim, the MIP films were electrochemically synthesized by varying the concentration of ETP between  $0.1 \times 10^{-4}$  and  $5.0 \times 10^{-4}$  M in the polymerization mixture. As shown in Figure 2(c), the sensitivity of MIP/GCE was found to increase as the ETP concentration grows in the polymerization mixture, reach maximum with the concentration of  $3.0 \times 10^{-4}$  M, and vary slightly afterward. As the template concentration increases in the polymerization mixture, a great number of specific cavities for ETP were generated within the polymer network. However, an overload of template molecules trapped inside the polypyrrole matrix often leads to very thick MIP films and results in poor access to the recognition sites [28]. Therefore, the concentration of ETP corresponding to the highest analytical response of MIP/GCE sensor was found to be  $3.0 \times 10^{-4}$  M and was chosen as the optimum.

It was also reported that the recorded analytical response of the MIP modified sensor is dependent on the rebinding process, consequently to the incubation time during the analytical measurement [41]. Under the optimized conditions, experiments were carried out by immersing the MIP/GCE sensor in 0.05 M BRB solution of pH 4.0 containing  $5.0 \times 10^{-6}$  M of ETP. The rebinding time was then varied from 1 to 20 min and the corresponding DPV voltammograms were recorded. The results pointed out that the MIP sensor exhibited a fast response time within almost 5 min. Above 5 min, no further signal increase was observed. This finding can be assigned to the lower mass-transfer resistance of the thin electrodeposited MIP film [41].

**3.2.4. Influence of the Number of Cycles.** The recognition ability of the electrochemical sensor could be affected by the thickness of the molecularly imprinted polypyrrole film. This fact is a result of the proportionality between the thickness of the MIP film and the scan number applied during the electropolymerization operation [38]. For this purpose, experiments were carried out in order to vary the number of cycles from 2 to 8 during the electropolymerization process, taking into account the optimum conditions determined previously. The analytical response of the MIP/GCE sensor first increased substantially with the cycle number up to 4 and then decreased considerably with further increase of cycle number (Figure 2(d)). The MIP coated electrode produced at lower number of cycles exhibited less sensitivity; this behavior could be attributed to the small number of recognition sites formed in the polymer matrix. On the other hand, further applied cycles could lead to the formation of thicker MIP films with less accessible recognition sites. The highest current difference for ETP at MIP and NIP modified GCEs was obtained by applying 4 cycles in the electropolymerization process.

**3.3. Characterization of the Developed MIP/GCE Sensor.** NIP and MIP films were characterized before and after the removal of ETP molecules by ATR-FTIR spectroscopy in order to control the effective embodiment of ETP molecules into the overoxidized polypyrrole network. Deformation vibrations associated with the pyrrole ring C-H and C-N bonds were observed at around  $774 \text{ cm}^{-1}$  and  $1287 \text{ cm}^{-1}$ , respectively, in all recorded spectra (Figure 3). The vibrations attributed to the C-N and C=C bonds of the pyrrole ring were observed at  $1527 \text{ cm}^{-1}$ . These bands correspond to major vibrations attributed to polypyrrole and are in agreement with those previously published in the literature [42], confirming the successful electrochemical synthesis of polypyrrole on the surface of GCE. Compared with the NIP spectra, the MIP spectra (Figure 3(b)) exhibited the characteristic absorption peaks of ETP at 901, 1090, 1366, 1479, and  $2860 \text{ cm}^{-1}$  corresponding, respectively, to AR-CH, AR-OH functional groups, -C-O from  $-\text{OCH}_3$ , OH, and  $\text{CH}_2$  stretching [43]. These data ascertain further evidence on the successful incorporation of ETP into the polymer network. Besides, ETP characteristic peaks disappeared totally after overoxidation (Figure 3(c)) which reveals the effectiveness of the overoxidation process

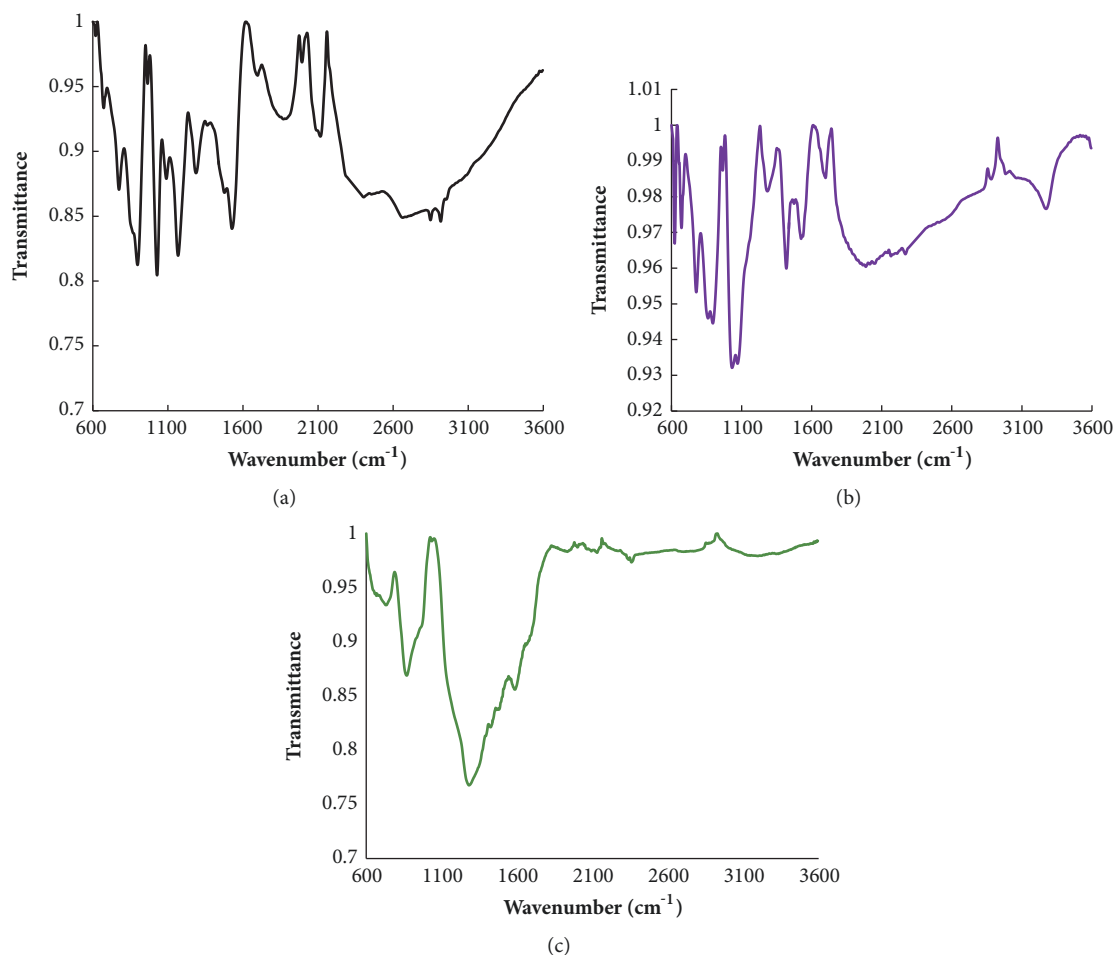


FIGURE 3: FTIR spectra of (a) NIP film, (b) MIP film, and (c) overoxidized MIP film.

in extracting the template molecules from the polypyrrole matrix. The absorption band observed at  $1660\text{ cm}^{-1}$  in the spectra of the overoxidized MIP film was associated with the elongation vibration of carbonyl group. This result affirms the presence of carbonyl groups in the matrix of the overoxidized polypyrrole because of the nucleophilic attack by the hydroxyl ions during the extraction process.

AFM tapping mode imaging was employed in this study to further investigate the morphological change that occurred on the surfaces of NIP and MIP films before and after the overoxidation process. Figure 4 displays 3D surface topography of the investigated films. Root mean squared roughness ( $R_q$ ) and average roughness ( $R_a$ ) were used to compare the different samples. It was found that the MIP film has a greater roughness ( $R_a = 177.62\text{ nm}$ ;  $R_q = 134.32\text{ nm}$ ) in comparison with the NIP film ( $R_a = 73.93\text{ nm}$ ;  $R_q = 92.55\text{ nm}$ ). This could be attributed to the creation of many aggregates on the surface of MIP modified electrode succeeding the inclusion of ETP molecules into the overoxidized polypyrrole network. Furthermore, it may also be related to the formation of new intermolecular interactions between ETP molecules and the polymeric matrix. It is worth noting that the overoxidized MIP film was found to be rougher than the MIP film obtained

immediately after the electropolymerization operation ( $R_a = 242\text{ nm}$ ;  $R_q = 330\text{ nm}$ ). This finding could be explained by the structural rearrangement during the overoxidation process, which leads to the introduction of new carboxyl and carbonyl groups in the polypyrrole network with simultaneous release of ETP molecules.

**3.4. Evaluation of the MIP Analytical Performance.** Figure 5 displays differential pulse voltammograms of  $0.05\text{ M}$  BRB solution of pH 4.0 containing increasing quantities of ETP that yielded well-defined anodic peaks at  $0.89\text{ V}$  versus SCE. The plot of the analytical response of MIP/GCE sensor, measured as the peak current, versus the respective concentration of ETP was found to be linear in the concentration range from  $5.0 \times 10^{-7}$  to  $1.0 \times 10^{-5}\text{ M}$  and was represented by the linear equation:  $I\ (\mu\text{A}) = 6.0393 \times [\text{ETP}] + 0.2307$ ,  $R^2 = 0.999$  (inset of Figure 5). The limit of detection (LOD) and limit of quantification (LOQ) were calculated as  $(3\sigma/m)$  and  $(10\sigma/m)$ , respectively, where  $\sigma$  is the standard deviation of the intercept and  $m$  is the slope of the calibration plot. The calculated LOD and LOQ were found to be  $2.8 \times 10^{-9}\text{ M}$  and  $9.24 \times 10^{-9}\text{ M}$ , respectively. The method precision was checked by

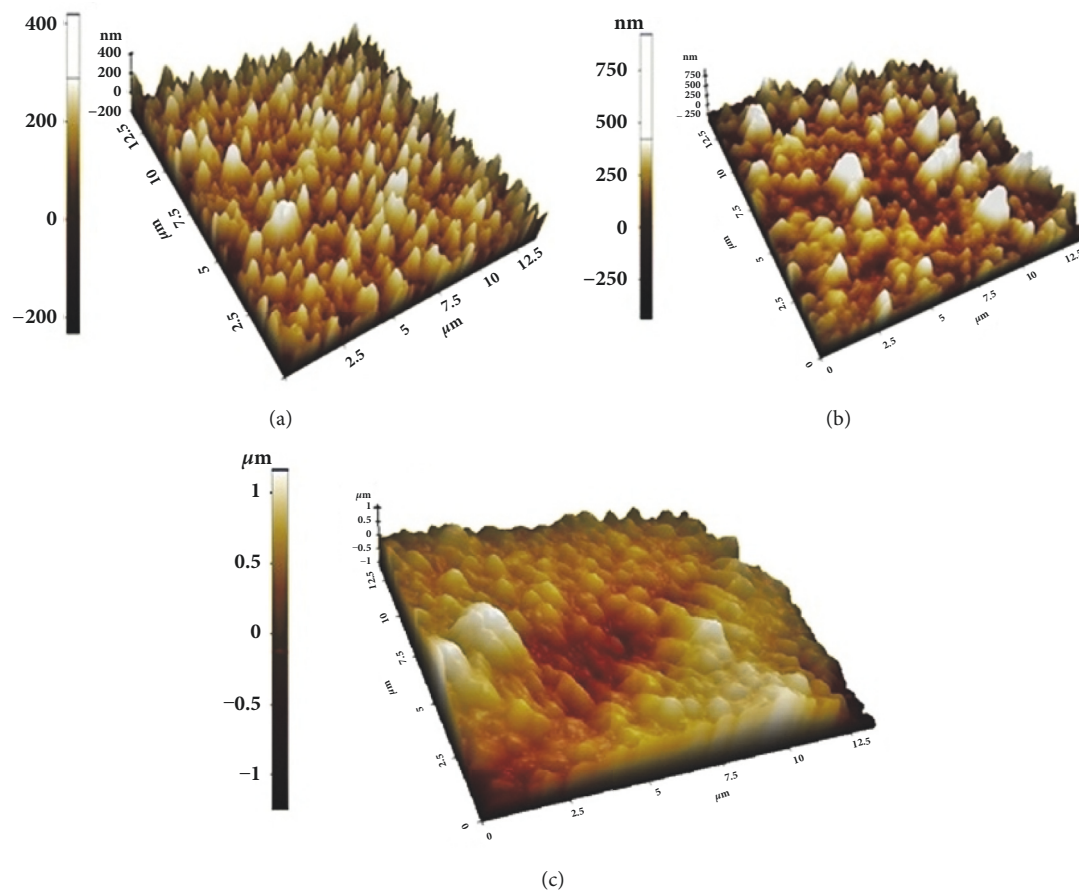


FIGURE 4: 3D AFM tapping mode images (12.5 μm × 12.5 μm) corresponding to (a) NIP film, (b) MIP film, and (c) overoxidized MIP film.

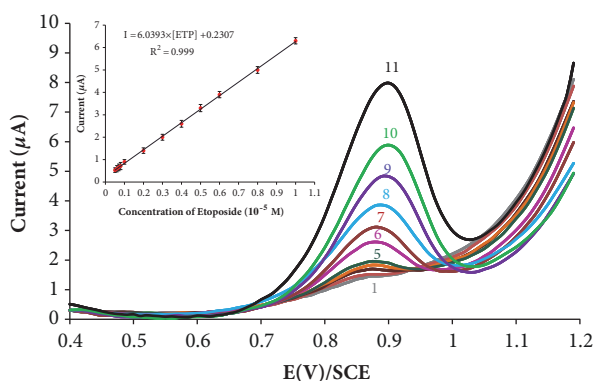


FIGURE 5: DP voltammograms of MIP/GCE sensor for different ETP concentrations: (1)  $5.0 \times 10^{-7}$  M; (2)  $6.0 \times 10^{-7}$  M; (3)  $7.0 \times 10^{-7}$  M; (4)  $8.0 \times 10^{-7}$  M; (5)  $1.0 \times 10^{-6}$  M; (6)  $2.0 \times 10^{-6}$  M; (7)  $3.0 \times 10^{-6}$  M; (8)  $4.0 \times 10^{-6}$  M; (9)  $6.0 \times 10^{-6}$  M; (10)  $8.0 \times 10^{-6}$  M; (11)  $1.0 \times 10^{-5}$  M. Experimental conditions: scan rate:  $10 \text{ mVs}^{-1}$ ; pulse amplitude: 50 mV; and pulse width: 20ms. The inset shows the calibration curve. Error bars represent the standard deviation of three independent measurements.

repeatedly ( $n=6$ ) measuring a standard solution containing  $5.0 \times 10^{-6}$  M ETP within a day and over six consecutive days. The average relative standard deviations (RSD) for

intra- and interday measurements were found to be 0.84 and 2.46%, respectively. The MIP based electrochemical sensor was stored in air at room temperature while not used; its stability was investigated by measuring the signal of  $5.0 \times 10^{-6}$  M ETP by DPV. It was found that there was almost 15% decrease of the peak current response after one week. These results reveal that the developed modified MIP sensor has both good stability and satisfactory reproducibility.

The robustness of the electroanalytical method is a measure of its ability to remain unaffected when perturbed by slight but deliberate variations in its method parameters and gives proof of its reliability during normal usage. In the present study, the influence of small variations of pH ( $4.0 \pm 0.1$ ) and Britton-Robinson concentration ( $0.05 \text{ M} \pm 0.01 \text{ M}$ ) on percentage recovery and relative standard deviation (% RSD) was evaluated by determination of  $5.0 \times 10^{-6}$  M ETP. In each experiment, only one parameter was changed. As shown in Table S.1 (Supplementary Material), the experimental results including the recovery values and relative standard deviations (% RSD) were insignificantly influenced by small changes in operational parameters. The recovery values and relative standard deviations were insignificantly influenced by small changes in operational parameters. Therefore, the proposed MIP/GCE sensor was considered reliable for the determination of ETP and can be regarded robust. The

TABLE 1: Effect of excipients on the differential pulse voltammetric response at the MIP/GCE sensor.

Interfering molecule	Concentration ( $10^{-6}$ M) <sup>a</sup>	Signal increase (%) <sup>b</sup>	R.S.D. (%) (n=3)
Benzyl Alcohol	0.8	1.47	1.17
	2	1.56	1.11
	5	1.61	1.44
	8	1.76	1.02
Citric Acid	0.8	1.13	0.88
	2	1.39	1.24
	5	1.56	1.55
	8	1.73	1.45
Polysorbate 80	0.8	1.11	0.69
	2	2.75	0.37
	5	3.16	1.67
	8	3.33	0.93
Macrogl 300	0.8	1.14	1.66
	2	1.98	0.75
	5	2.49	0.66
	8	2.66	1.31

<sup>a</sup>Concentration added to 10.0 mL of  $5.0 \times 10^{-6}$  M Etoposide solution.

<sup>b</sup>Percent increase of analytical response after the addition of interfering molecule.

ruggedness of the developed method was estimated by applying the proposed modified sensor to assay of  $5.0 \times 10^{-6}$  M ETP using the same equipment by two different analysts from the same laboratory under the same optimized conditions on different days. The results were found to be reproducible and % RSD values were calculated as 0.42 and 0.59% for the first and second analyst, respectively. The obtained data were compared statistically using Student's t-test and F-test. The calculated values of t- and F-tests ( $t_c = 0.72$  and  $F_c = 1.18$ ,  $n = 6$ ) were less than the theoretical values further ascertaining that there was no significant statistical differences between the analyses (confidence level 95%). Consequently, the proposed method could be considered robust.

**3.5. Interference Studies.** The selectivity of the MIP film was evaluated by exposing the modified GCE to  $5.0 \times 10^{-6}$  M ETP standard solution in the presence of increasing concentrations of additives (benzyl alcohol, citric acid, polysorbate 80, and macrogl 300). These substances are usually present as excipients in the injectable dosage forms and may interfere with the determination of ETP through conventional methods. The DPV response of each MIP/GCE sensor was recorded before and after the addition of each interfering molecule to the drug solution, and the percentage of signal change was calculated. As shown in Table 1, no significant interference could be detected by the addition of four levels of interfering molecules varying from 0.8 to  $8.0 \times 10^{-6}$  M. All the percentages obtained were lower than 3.4%. This indicates that excipients do not interfere with the determination of ETP and demonstrates the high selectivity of MIP/GCE sensor toward ETP molecules by means of shape selection and size of functional groups.

The selectivity of the MIP/GCE sensor has also been tested in biological fluids such as plasma and blood serum as well as urine in the presence of ETP metabolites which are ETP quinone and ETP catechol (Figure S.2, Supplementary Material). The biological fluids were spiked with  $5.0 \times 10^{-6}$  M ETP standard solution, and increasing concentrations of metabolites were added to the solution. The low percentages of signal increase (Table 2) demonstrate the high resistance of the MIP modified sensor against the interference effects of the matrices compounds. However, experimental results indicated that the response of ETP at the NIP modified electrodes was affected by these interferents. These results are an irrefutable proof of a possible direct use of the modified MIP/GCE sensor for the analysis of ETP in biological fluids.

**3.6. Application to Real Samples.** In order to demonstrate the practical usage of the MIP modified sensor in the pharmaceutical sample analysis, it was used to detect ETP in Etoposide Mylan® injection. Moreover, to test the reliability of this method, Etoposide Mylan® was also determined with a previous reference HPLC method [11]. Results summarized in Table 3 showed that the values obtained by the MIP/GCE sensor fitted well with those found by the HPLC method and compared fairly well with the content marked in the label. These results reveal the accuracy and reliability of the proposed MIP/GCE sensor in the determination of ETP in injection solution. The obtained results were further compared statistically using Student's t-test. The calculated t-value did not exceed the theoretical value, confirming that there is no considerable difference between the compared methods (confidence limit 95%).

To further explore the practical application of the developed sensor, determination of ETP in biological human fluids



TABLE 2: Effect of metabolites on the differential pulse voltammetric response at the MIP/GCE sensor in biological human fluids.

Biological fluid	Metabolite	Concentration ( $10^{-6}$ M) <sup>a</sup>	Signal increase (%) <sup>b</sup>	RSD (%) n=3
Plasma	ETP Quinone	2	0.39	0.38
		5	0.41	0.11
		8	0.99	0.42
	ETP Catechol	2	0.92	0.60
		5	1.01	0.46
		8	1.04	1.21
Serum	ETP Quinone	2	0.88	0.55
		5	0.96	1.21
		8	0.99	0.29
	ETP Catechol	2	0.68	0.73
		5	1.74	0.43
		8	1.90	0.28
Urine	ETP Quinone	2	0.44	0.61
		5	0.58	1.42
		8	0.61	0.78
	ETP Catechol	2	0.93	0.81
		5	1.23	1.09
		8	1.31	0.91

<sup>a</sup>Spiked concentration to 10.0 mL of  $5.0 \times 10^{-6}$  M ETP solution.

<sup>b</sup>Percent increase of analytical response following the addition of metabolite.

TABLE 3: Determination of ETP in injectable solution (n=6) using the proposed MIP/GCE sensor and reported HPLC method [11].

	Etoposide Mylan®	
	MIP/GCE sensor	HPLC
Mean (mg/5 mL)	20.06	20.00
RSD%	1.07	0.91
t-test (significance level 0.05; n=6)	Calculated value 0.415 < theoretical value 2.571	

\*Claimed concentration is 20.0 mg/5.0 mL.

(serum, plasma and urine samples) was carried out. The obtained results are summarized in Table 4 and indicate that the composition of all studied biological matrices has no significant influence on the sensing of ETP. The values of recoveries were ranged from 98.50 to 100.25%, and % RSD ranged from 0.35 to 1.48, indicating that the proposed modified sensor has good accuracy and great potential for practical application for the analysis of ETP in real samples.

#### 4. Conclusion

In this study, the fabrication of a new electropolymerized molecularly imprinted overoxidized polypyrrole for direct ETP determination in injectable dosage forms and biological fluids was investigated. To the best of our knowledge, this work is the first report on the combination of the molecular imprinting technique and the electrochemical detection for the quantification of ETP. In comparison with the analytical performances of previously reported ETP sensors published in the scientific literature (Table 5), the modified MIP/GCE sensor displayed the lowest limit of detection and possessed

great resistance against potentially interfering molecules present in biological fluids and injectable dosage forms. Each method also has its limitations and advantages, which would provide a specific need in analysis. To get the best response of ETP at the modified sensor, some important conditions influencing the preparation of MIP/GCE and the electrochemical oxidation ETP have been optimized. Under the optimum conditions, there was a good linear relationship between the anodic peak current and the concentration of ETP in the range of  $5.0 \times 10^{-7}$  –  $1.0 \times 10^{-5}$  M with a detection limit of  $2.8 \times 10^{-9}$  M. The modified MIP/GCE sensor, besides its rapidity, simplicity, and low cost, revealed a good selectivity in the determination of ETP and has proved to be promising in the measurements of ETP in clinical samples as well as pharmaceutical formulations.

#### Data Availability

The data used to support the findings of this study are available from the corresponding author upon request.

TABLE 4: Recovery of Etoposide from the biological human fluids.

Biological fluid	Added amount ( $10^{-6}$ M)	Found amount ( $10^{-6}$ M)	Recovery (%)	RSD (%) (n=3)
Urine	2	1.98	99.00	0.35
	4	4.01	100.25	0.51
Plasma	2	1.97	98.50	1.26
	4	3.98	99.50	1.48
Serum	2	1.99	99.50	0.64
	4	3.95	98.75	0.79

TABLE 5: Comparison of the present work and previous electrochemical studies for the determination of ETP.

Electrode	Technique	LCR (M)	LOD (M)	Application	Ref.
CPE	DPV	$2.5 \times 10^{-7}$ – $2.5 \times 10^{-5}$	$1.0 \times 10^{-7}$	Serum	[22]
MWCNT/GCE	AdsDPV	$2.0 \times 10^{-8}$ – $2.0 \times 10^{-6}$	$5.4 \times 10^{-9}$	Pharmaceuticals	[23]
GCE	DPV	$0.06 \times 10^{-6}$ – $10 \times 10^{-6}$	$0.017 \times 10^{-6}$	Cancer cells	[26]
GCE/CQDs	DPV	$0.02 \times 10^{-6}$ – $10 \times 10^{-6}$	$0.005 \times 10^{-6}$	Cancer cells	[26]
GCE/MIP	DPV	$5.0 \times 10^{-7}$ – $1.0 \times 10^{-5}$	$2.8 \times 10^{-9}$	Serum, plasma, urine and pharmaceuticals	<b>This work</b>

**Abbreviations:** CPE: carbon paste electrode; MWCNT: multiwalled carbon nanotubes; CQDs: carbon quantum dots; AdsDPV: adsorptive stripping differential pulse voltammetry; LCR: linear concentration range; LOD: limit of detection.

## Conflicts of Interest

The authors declare no financial, academic, commercial, political, or personal conflicts of interest.

## Supplementary Materials

**FIGURE S.1:** (A) cyclic voltammograms taking during the overoxidation operation ([NaOH]: 0.1 M; scan rate:  $50 \text{ mVs}^{-1}$ ; number of scans: 40), (B) evolution of the concentration of ETP released from the polymeric matrix during its removal with the number of cycles applied during the overoxidation process. Error bars represent standard deviations of three independent measurements. **FIGURE S.2:** structures of Etoposide, Etoposide catechol, and Etoposide quinone. **TABLE S.1:** effect of small variations in BRB concentration and pH on recovery of  $5.0 \times 10^{-6}$  M of Etoposide. (*Supplementary Materials*)

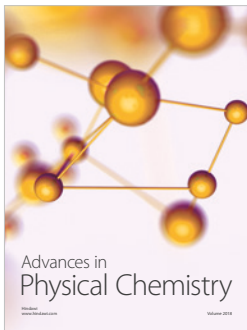
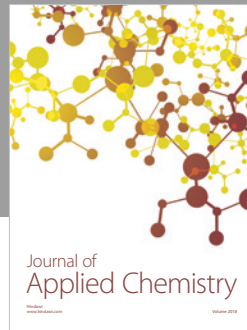
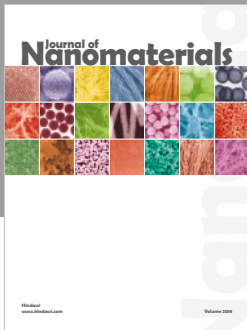
## References

- [1] R. T. Dorr and D. D. Von Hoff, *Cancer Chemotherapy Handbook*, CT: Appleton & Lange, Norwalk, Conn, USA, 2nd edition, 1994.
- [2] D. H. Johnson, J. D. Hainsworth, K. R. Hande, and F. Anthony Greco, "Current status of etoposide in the management of small cell lung cancer," *Cancer*, vol. 67, no. 1, pp. 231–244, 1991.
- [3] T. Groh, J. Hrabeta, J. Poljakova, T. Eckschlagler, and M. Stiborova, "Impact of histone deacetylase inhibitor valproic acid on the anticancer effect of etoposide on neuroblastoma cells," *Neuroendocrinology Letters*, vol. 33, no. 3, pp. 16–24, 2012.
- [4] S. Pang, N. Zheng, C. A. Felix, J. Scavuzzo, R. Boston, and I. A. Blair, "Simultaneous determination of etoposide and its catechol metabolite in the plasma of pediatric patients by liquid chromatography/tandem mass spectrometry," *Journal of Mass Spectrometry*, vol. 36, no. 7, pp. 771–781, 2001.
- [5] K. G. Blume, S. J. Forman, M. R. O'Donnell et al., "Total body irradiation and high-dose etoposide: A new preparatory regimen for bone marrow transplantation in patients with advanced hematologic malignancies," *Blood*, vol. 69, no. 4, pp. 1015–1020, 1987.
- [6] Y. Pommier, G. Capranico, A. Orr, and K. W. Kohn, "Distribution of topoisomerase II cleavage sites in simian virus 40 DNA and the effects of drugs," *Journal of Molecular Biology*, vol. 222, no. 4, pp. 909–924, 1991.
- [7] R. E. Durand and J. H. Goldie, "Interaction of etoposide and cisplatin in an in vitro tumor model," *Cancer Treatment Reports*, vol. 71, no. 7-8, pp. 673–679, 1987.
- [8] F. Kanzawa, K. Nisnio, K. Fukuoka, M. Fukuda, T. Kunimoto, and N. Saijo, "Evaluation of synergism by a novel three-dimensional model for the combined action of cisplatin and etoposide on the growth of a human small-cell lung-cancer cell line, SBC-3," *International Journal of Cancer*, vol. 71, no. 3, pp. 311–319, 1997.
- [9] L. Brunton, J. Lazo, and K. Parker, *Goodman & Gilman's: The Pharmacological Basis of Therapeutics*, Mc Graw Hill, New York, NY, USA, 11th edition, 2001.
- [10] M. C. Pigatto, D. L. Mossmann, and T. D. Costa, "HPLC-UV method for quantifying etoposide in plasma and tumor interstitial fluid by microdialysis: Application to pharmacokinetic studies," *Biomedical Chromatography*, vol. 29, no. 4, pp. 529–536, 2015.
- [11] M. Munawar Hayat, M. Ashraf, Nisar-Ur-Rehman et al., "HPLC determination of etoposide in injectable dosage forms," *Journal of the Chilean Chemical Society*, vol. 56, no. 4, pp. 881–883, 2011.
- [12] R. Zhou, M. Frostvik-Stolt, and E. Liliemark, "Determination of etoposide in human plasma and leukemic cells by high-performance liquid chromatography with electrochemical detection," *Journal of Chromatography B: Biomedical Sciences and Applications*, vol. 757, no. 1, pp. 135–141, 2001.

- [13] Y.-L. Cao, X.-L. Du, Z. Zhu, and Q. Fu, "HPLC assay for determination of etoposide in human plasma," *Chinese Pharmaceutical Journal*, vol. 46, no. 11, pp. 857–859, 2011.
- [14] M. Ashraf, M. M. Hayat, F.-U. Nasim, I. Ahmad, M. Saleem, and J. Rahman, "Development and validation of RP-HPLC method for the simultaneous determination of etoposide and cisplatin and its application in quality control of injectable dosage forms," *Journal of The Chemical Society Of Pakistan*, vol. 34, no. 2, pp. 321–325, 2012.
- [15] M. Snehaltha, B. Girish, K. Venugopal, and R. N. Saha, "Validated, reversed phase high performance liquid chromatography method for the estimation of etoposide in bulk and formulations," *Indian Journal of Pharmaceutical Education and Research*, vol. 41, no. 4, p. 347, 2007.
- [16] O. T. Fahmy, M. A. Korany, and H. M. Maher, "High performance liquid chromatographic determination of some co-administered anticancer drugs in pharmaceutical preparations and in spiked human plasma," *Journal of Pharmaceutical and Biomedical Analysis*, vol. 34, no. 5, pp. 1099–1107, 2004.
- [17] R. Saadati and S. Dadashzadeh, "Simple and efficient HPLC-UV quantitation of etoposide and its cis-isomer in rat micro-volume plasma and tissue samples: Application to pharmacokinetic and biodistribution studies," *Journal of Liquid Chromatography & Related Technologies*, vol. 34, no. 18, pp. 2130–2148, 2011.
- [18] C.-L. Chen and F. M. Uckun, "Highly sensitive liquid chromatography-electrospray mass spectrometry (LC-MS) method for the determination of etoposide levels in human serum and plasma," *Journal of Chromatography B: Biomedical Sciences and Applications*, vol. 744, no. 1, pp. 91–98, 2000.
- [19] N. Akhtar, S. Talegaonkar, R. K. Khar, and M. Jaggi, "A validated stability-indicating LC method for estimation of etoposide in bulk and optimized self-nano emulsifying formulation: Kinetics and stability effects," *Saudi Pharmaceutical Journal*, vol. 21, no. 1, pp. 103–111, 2013.
- [20] S. L. Prabu, S. Shah Nawaz, C. D. Kumar, S. G. Vasantharaju, and N. Sivagurunathan, "Spectrofluorimetric method for determination of etoposide in bulk and pharmaceutical dosage forms," *Indian Drugs Journal*, vol. 46, no. 12, pp. 58–60, 2009.
- [21] N. Y. Ragozina, M. Pütz, S. Heissler, W. Faubel, and U. Pyell, "Quantification of etoposide and etoposide phosphate in human plasma by micellar electrokinetic chromatography and near-field thermal lens detection," *Analytical Chemistry*, vol. 76, no. 13, pp. 3804–3809, 2004.
- [22] A.-E. Radi, N. Abd-Elghany, and T. Wahdan, "Electrochemical study of the antineoplastic agent etoposide at carbon paste electrode and its determination in spiked human serum by differential pulse voltammetry," *Chemical & Pharmaceutical Bulletin*, vol. 55, no. 9, pp. 1379–1382, 2007.
- [23] B. Bozal-Palabiyik, B. Dogan-Topal, B. Uslu, A. Can, and S. A. Ozkan, "Sensitive voltammetric assay of etoposide using modified glassy carbon electrode with a dispersion of multi-walled carbon nanotube," *Journal of Solid State Electrochemistry*, vol. 17, no. 11, pp. 2815–2822, 2013.
- [24] D. Eskiköy Bayraktepe, T. Yanardag, Z. Yazan, and A. Aksüt, "Voltammetric determination of etoposide by using Sepiolite clay modified electrode and its interaction with DNA," *Revue Roumaine de Chimie*, vol. 60, no. 4, pp. 287–295, 2015.
- [25] Z. Heger, A. Moulick, H. V. Nguyen et al., "Characterization of multi-walled carbon nanotubes double-functionalization with cytostatic drug etoposide and phosphorothioate oligodeoxynucleotides," *International Journal of Electrochemical Science*, vol. 10, no. 9, pp. 7707–7719, 2015.
- [26] H. V. Nguyen, L. Richtera, A. Moulick et al., "Electrochemical sensing of etoposide using carbon quantum dot modified glassy carbon electrode," *Analyst*, vol. 141, no. 9, pp. 2665–2675, 2016.
- [27] B. B. Prasad, A. Kumar, and R. Singh, "Molecularly imprinted polymer-based electrochemical sensor using functionalized fullerene as a nanomediator for ultratrace analysis of primaquine," *Carbon*, vol. 109, pp. 196–207, 2016.
- [28] H. Hrichi, L. Monser, and N. Adhoum, "A novel electrochemical sensor based on electropolymerized molecularly imprinted poly(aniline-co-anthranilic acid) for sensitive detection of amlodipine," *Journal of Electroanalytical Chemistry*, vol. 805, pp. 133–145, 2017.
- [29] A. Florea, O. Hosu, B. Ciui, and C. Cristea, "Molecularly imprinted polymer-based sensors for biomedical and environmental applications," in *Advanced Molecularly Imprinting Materials*, A. Tiwari and L. Uzun, Eds., Scriver Publishing, NJ, USA, 2016.
- [30] M. C. Blanco-Lopez, S. Gutierrez-Fernandez, M. J. Lobo-Castanon, A. J. Miranda-Ordieres, and P. Tunon-Blanco, "Electrochemical sensors based on molecularly imprinted polymers," *TrAC Trends in Analytical Chemistry*, vol. 23, no. 1, pp. 36–48, 2004.
- [31] J. Nemeč, "Epipodophyllotoxinquinone glucoside derivatives, method of production and use," U.S. Patent 4609644, 1986.
- [32] M. V. Relling, R. Evans, C. Dass, D. M. Desiderio, and J. Nemeč, "Human cytochrome P450 metabolism of teniposide and etoposide," *The Journal of Pharmacology and Experimental Therapeutics*, vol. 261, no. 2, pp. 491–496, 1992.
- [33] S. Sun, M. Zhang, Y. Li, and X. He, "A molecularly imprinted polymer with incorporated Graphene oxide for electrochemical determination of quercetin," *Sensors*, vol. 13, no. 5, pp. 5493–5506, 2013.
- [34] I. Rodríguez, B. R. Scharifker, and J. Mostany, "In situ FTIR study of redox and overoxidation processes in polypyrrole films," *Journal of Electroanalytical Chemistry*, vol. 491, no. 1–2, pp. 117–125, 2000.
- [35] L. Songjun, G. Yi, A. S. A. Piletsky, and J. Lunec, *Molecularly Imprinted Sensors: Overview and Applications*, Elsevier, Amsterdam, Netherlands, 2012.
- [36] S. Varghese, K. P. Prathish, and T. P. Rao, "Molecularly imprinted conducting polymer film based aqueous amino acid sensors," US patent 9239311 B2, 2012.
- [37] H. Shiigi, H. Yakabe, M. Kishimoto et al., "Molecularly Imprinted Overoxidized Polypyrrole Colloids: Promising Materials for Molecular Recognition," *Microchimica Acta*, vol. 143, no. 2–3, pp. 155–162, 2003.
- [38] A.-E. Radi and I. Abd-Elaziz, "A halofuginone electrochemical sensor based on a molecularly imprinted polypyrrole coated glassy carbon electrode," *Analytical Methods*, vol. 7, no. 19, pp. 8152–8158, 2015.
- [39] J. Liu, H. Tang, B. Zhang et al., "Electrochemical sensor based on molecularly imprinted polymer for sensitive and selective determination of metronidazole via two different approaches," *Analytical and Bioanalytical Chemistry*, vol. 408, no. 16, pp. 4287–4295, 2016.
- [40] B. Tian and G. Zerbi, "Lattice-Dynamics and Vibrational Spectra of Polypyrrole," *The Journal of Chemical Physics*, vol. 92, no. 6, pp. 3886–3891, 1990.
- [41] A.-E. Radi, N. Abd El-Ghany, and T. Wahdan, "Voltammetric Determination of Flunixin on Molecularly Imprinted Polypyrrole Modified Glassy Carbon Electrode," *Journal of Analytical*

*Methods in Chemistry*, vol. 2016, Article ID 5296582, 7 pages, 2016.

- [42] K. Arora, A. Chaubey, R. Singhal et al., "Application of electrochemically prepared polypyrrole-polyvinyl sulphonate films to DNA biosensor," *Biosensors and Bioelectronics*, vol. 21, no. 9, pp. 1777–1783, 2006.
- [43] B. R. Jasti, J. Du, and R. C. Vasavada, "Characterization of thermal behavior of etoposide," *International Journal of Pharmaceutics*, vol. 118, no. 2, pp. 161–167, 1995.



Hindawi

Submit your manuscripts at  
[www.hindawi.com](http://www.hindawi.com)

